ANALYSIS OF DIFFUSION DELAY IN A LAYERED MEDIUM

Application to Heat Measurements from Muscle

SUSAN H. GILBERT* AND RICHARD T. MATHIAS‡
*Departments of *Anatomical Sciences, and ‡Physiology and Biophysics, State University of New York at Stony Brook, Stony Brook, New York 11794*

ABSTRACT An analysis is presented of diffusional delays in one-dimensional heat flow through a medium consisting of several layers of different materials. The model specifically addresses the measurement of heat production by muscle, but diffusion of solute or conduction of charge through a layered medium will obey the same equations. The model consists of a semi-infinite medium, the muscle, in which heat production is spacially uniform but time varying. The heat diffuses through layers of solution and insulation to the center of the thermal element where heat flow is zero. Using Laplace transforms, transfer functions are derived for the temperature change in the center of the thermopile as a function of the temperature at any interface between differing materials or as a function of heat production in the muscle. From these transfer functions, approximate analytical expressions are derived for the time constants which scale the early and late changes in the central temperature. We find that the earliest temperature changes are limited by the diffusivities of the materials, whereas the approach to steady state depends on the total heat capacity of the system and the diffusivity of muscle. Hill (1937) analyzed a similar geometry by modeling the layered medium as a homogeneous system with an equivalent half thickness. We show that his analysis was accurate for the materials in his system. In general, however, and specifically with regard to modern thermopiles, a homogeneous approximation will lead to significant errors.

We compare responses of different thermopiles to establish the limits of time resolution in muscle heat records and to correct them for diffusional delays. Using numerical techniques, we invert the Laplace transforms and show the time course of the temperature changes recorded by different instruments in response to different patterns of heat production.

INTRODUCTION

There are many situations in which physiologically interesting fluxes occur through layers of material. Examples include the diffusion of solute or conduction of ions from one side of an epithelium to the other or the flow of heat from one body to another. The solution of such problems is algebraically tedious because it involves satisfying two sets of boundary conditions per layer. This complexity makes it difficult to understand physically what is happening, so investigators frequently ignore the layers and analyze the flux as if the medium were homogeneous with a set of effective parameters. However, we find that no single set of effective parameters will describe the entire time course when the medium is actually layered.

Here we examine in detail the flux of heat from a semi-infinite source, through three finite layers to a central plane where the heat flow is zero. This geometry represents the experimental measurement of heat production in muscle, where a small thermopile is sandwiched between two relatively large muscles, hence, by symmetry, there is no heat flux at the center. Laplace transforms are used to derive a series of transfer functions relating the temperature at each interface to that at the next and to the rate of heat production.

Analytic expressions are derived for the time course of the initial rate of temperature change and final approach to steady state after an impulse in heat production. Each expression has the same form, regardless of the number of layers, hence these phases of the response can be extrapolated to describe a general system of n layers.

GLOSSARY

a	half-thickness of layer 0 (thermal junctions), cm
b	thickness of layer 1 (insulation), cm
c	thickness of layer 2 (insulation or inert fluid/tissue), cm
C	heat capacity per unit mass, J/deg-g
k	thermal diffusivity, cm^2/s
K	thermal conductivity, J/cm-s-deg, or W/cm-deg
q	rate of heat production, $J/s\text{-}cm^3$
s	Laplace transform variable, s^{-1}
t	time, s

Address all correspondence to Susan Gilbert, Department of Anatomical Sciences, SUNY Stony Brook, Stony Brook, NY 11794

T	temperature, deg C
V	heat capacity per unit volume = ρC, J/deg-cm^3
x	distance, cm
$\gamma_n^2 = s/k_n$	for nth layer
ρ	density, g/cm^3

Subscripts

n –	0: thermal junctions
	1: insulation
	2: inert fluid/tissue
	3: muscle

THEORY

Muscle heat production is measured by sandwiching a thin thermopile between a pair of muscles. Current is produced when the temperature of thermal junctions in contact with the muscles changes with respect to junctions in contact with a heat sink of large thermal capacity. The speed of the measurements is limited by the time required for heat produced by the muscles to diffuse through intervening layers to the thermal junctions and change their temperature.

Fig. 1 illustrates the geometry of the system. The muscles and layers of insulation are symmetrical on each side of the thermal junctions. Since heat loss from the muscles and themopile to the surroundings occurs with a time constant of 20–30 s, it is insignificant at intervals of <1 s, and the muscles are assumed to lose heat only to layers 0, 1, and 2. The heat equation in regions 0–2 is

$$\frac{\partial T_n}{\partial t} = k_n \frac{\partial^2 T_n}{\partial x^2},$$

where $k_n = K_n/V_n$. First, the Laplace transform of the heat equation will be solved to obtain the transfer function relating the temperature at the thermal junctions to heat production by the muscles. We then numerically invert the transformed temperature using an IMSL subroutine (International Mathematical Statistical Libraries, Inc., Houston, Texas) and examine the responses of specific thermopiles to transient heat produced by the muscles.

The transformed heat equation in regions 0, 1, and 2 is

$$\frac{1}{\gamma_n^2}\frac{d^2T_n}{dx^2} - T_n = 0, \tag{1}$$

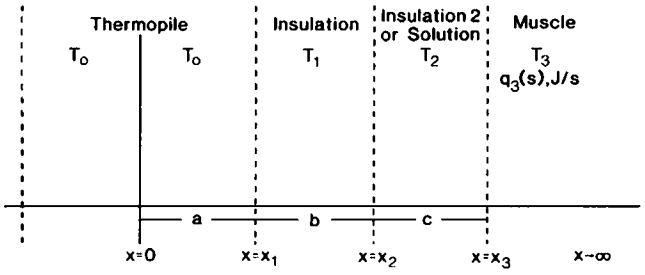

FIGURE 1 Geometry of heat diffusion barriers for a thermopile with a muscle mounted on each face. The layers are symmetrical on each side of a plane in the center of the thermal junctions, whose half-thickness is dimension *a*. Covering the couples are a layer of insulation (*thickness b*) and an additional layer of insulation or solution (thickness *c*).

where $\gamma_n^2 = s/k_n$. In the muscle (layer 3), uniform heat production at a rate $q_3(t)$ modifies the equation to

$$\frac{1}{\gamma_3^2}\frac{d^2T_3}{dx^2} - T_3 = -\frac{q_3(s)}{sV_3}. \tag{2}$$

The boundary conditions are

$$\text{symmetry:} \quad \frac{dT_0(0)}{dx} = 0 \tag{3}$$

$$\text{continuity of temperature:} \quad T_n(x_{n+1}) = T_{n+1}(x_{n+1}) \tag{4}$$

$$\text{continuity of heat flow:} \quad K_n \frac{dT_n(x_{n+1})}{dx} = K_{n+1}\frac{dT_{n+1}(x_{n+1})}{dx} \tag{5}$$

$$\text{infinite boundary:} \quad dT_3(\infty)dx = 0. \tag{6}$$

Define

$$T_0(0, s) = H_0(s)\, T_1(x_1, s) \tag{7}$$

$$T_1(x_1, s) = H_1(s) T_2(x_2, s) \tag{8}$$

$$T_2(x_2, s) = H_2(s) T_3(x_3, s) \tag{9}$$

$$T_3(x_3, s) = H_3(s)\frac{q_3(s)}{sV_3} \tag{10}$$

$$\frac{q_3(s)}{sV_3} \rightarrow \boxed{H_3(s)} \xrightarrow{T_3(x_3)} \boxed{H_2(s)} \xrightarrow{T_2(x_2)} \boxed{H_1(s)} \xrightarrow{T_1(x_1)} \boxed{H_0(s)} \rightarrow T_0(0, s).$$

Using these definitions and the requirement for continuity of temperature, we can write

$$T_0(x) = T_1(x_1)\frac{\cosh \gamma_0 x}{\cosh \gamma_0 a} \tag{11}$$

$$T_1(x) = T_2(x_2)\left[\cosh \gamma_1(x - x_1) + \frac{\cosh \gamma_1 b - H_1(s)}{\sinh \gamma_1 b}\sinh \gamma_1(x - x_1)\right] \tag{12}$$

$$T_2(x) = T_3(x_3)\left[\cosh \gamma_2(x - x_2) + \frac{\cosh \gamma_2 c - H_2(s)}{\sinh \gamma_2 c}\sinh \gamma_2(x - x_2)\right] \tag{13}$$

$$T_3(x) = \frac{q_3(s)}{V_3 s}\left[H_3(s)e^{-\gamma_3(x-x_3)} + 1 - e^{-\gamma_3(x-x_3)}\right]. \tag{14}$$

The continuity of heat flow condition allows us to specify the transfer functions

$$H_0(s) = \frac{1}{\cosh \gamma_0 a} \tag{15}$$

$$H_1(s) = \frac{1}{\cosh \gamma_1 b D_1(s)}, \tag{16}$$

$$H_2(s) = \frac{D_1(s)}{\cosh \gamma_2 c D_2(s)}, \tag{17}$$

$$H_3(s) = \frac{D_2(s)}{D_3(s)}, \tag{18}$$

where

$$D_1(s) = 1 + \frac{V_0\sqrt{k_0}}{V_1\sqrt{k_1}} \tanh \gamma_0 a \tanh \gamma_1 b \tag{19}$$

$$D_2(s) = \left[1 + \frac{V_0\sqrt{k_0}}{V_1\sqrt{k_1}} \tanh \gamma_0 a \tanh \gamma_1 b + \frac{V_0\sqrt{k_0}}{V_2\sqrt{k_2}} \tanh \gamma_0 a \tanh \gamma_2 c + \frac{V_1\sqrt{k_1}}{V_2\sqrt{k_2}} \tanh \gamma_1 b \tanh \gamma_2 c\right] \tag{20}$$

and

$$\begin{aligned} D_3(s) = 1 &+ \frac{V_0\sqrt{k_0}}{V_3\sqrt{k_3}}\tanh \gamma_0 a + \frac{V_1\sqrt{k_1}}{V_3\sqrt{k_3}}\tanh \gamma_1 b \\ &+ \frac{V_2\sqrt{k_2}}{V_3\sqrt{k_3}}\tanh \gamma_2 c + \frac{V_0\sqrt{k_0}}{V_1\sqrt{k_1}}\tanh \gamma_0 a \tanh \gamma_1 b \\ &+ \frac{V_0\sqrt{k_0}}{V_2\sqrt{k_2}}\tanh \gamma_0 a \tanh \gamma_2 c \\ &+ \frac{V_1\sqrt{k_1}}{V_2\sqrt{k_2}}\tanh \gamma_1 b \tanh \gamma_2 c \\ &+ \frac{V_0\sqrt{k_0}V_2\sqrt{k_2}}{V_1\sqrt{k_1}V_3\sqrt{k_3}}\tanh \gamma_0 a \tanh \gamma_1 b \tanh \gamma_2 c. \end{aligned} \tag{21}$$

By definition (Eqs. 7–10) the transfer functions $H_{0\text{-}3}$ operate successively on the input function $q_3(s)/(V_3 s)$, where $q_3(s)$ is the rate of volume heat production in J/cm^3-s and V_3 the volume thermal capacity of the muscle in $J/deg\text{-}cm^3$. As expected, the transfer function of any region 0–2 approaches unity as the region becomes infinitely thin:

$$\lim_{(x_{n+1}-x_n)\to 0} H_n(s) = 1. \tag{22}$$

The transfer function of the system is the product of the individual transfer functions

$$H(s) = H_3(s) \cdot H_2(s) \cdot H_1(s) \cdot H_0(s) \tag{23}$$

such that

$$T_0(0, s) = H(s) \cdot \frac{q_3(s)}{sV_3}. \tag{24}$$

From Eqs. 15–21 and 23

$$H(s) = \frac{1}{\cosh \gamma_0 a \cosh \gamma_1 b \cosh \gamma_2 c D_3(a, b, c, s)}, \tag{25}$$

where the fifth term of the denominator, $D_3(a, b, c, s)$, is given by Eq. 21.

RESULTS

Effects of Diffusivity and Thermal Capacity

Since the temperature in the thermal element is spatially not uniform, we compute the response from the average of the temperature.

$$\bar{T}_0(s) = \frac{1}{a}\int_0^a T_0(x, s)\, dx = \frac{\sinh \gamma_0 a}{\gamma_0 a} T_0(0, s). \tag{26}$$

However, given the parameters in Table I, the temperature at $x = 0$ is not significantly different from the averaged temperature. The thermopile's transformed step response, that is, the output resulting from an impulse in the rate of heat production (Δq_3) by the muscles, is

$$\bar{T}_0(s) = \frac{\sinh \gamma_0 a}{\gamma_0 a} H(s) \frac{\Delta q_3}{sV_3}. \tag{27}$$

The step response in the time domain consists of an initial rapidly rising phase followed by a long slow tail to the final value, as shown in Figs. 2–5 and described in detail below. These two phases are related to different physical properties of various thermopile layers.

The slope of the initial rising phase is most easily understood by examining the initial rate of change in $T_0(0, t)$. This can be evaluated by expanding the transformed equations in large s, then inverting the expression for $sT_0(0, s)$ as $s \to \infty$ to obtain $dT_0(0, t)/dt$ as $t \to 0$. The large s expansion is

$$\frac{\Delta q_3}{V_3} \to \boxed{A_{2,3}} \xrightarrow{T_3(x_3 s)} \boxed{A_{1,2}A_{0,1}2^3 e^{\sqrt{\tau_0 s}}} \to T_0(0, s),$$

where the constants, $A_{n,m}$, are given by

$$A_{n,m} = \frac{1}{1 + V_n\sqrt{k_n}/(V_m\sqrt{k_m})} \tag{28}$$

and the time constant is

$$\begin{aligned} \tau_0 &= \ell^2/k_{\text{eff}} \\ \ell &= a + b + c \\ k_{\text{eff}} &= 1\Big/\left(\frac{a}{\ell\sqrt{k_0}} + \frac{b}{\ell\sqrt{k_1}} + \frac{c}{\ell\sqrt{k_2}}\right)^2. \end{aligned} \tag{29}$$

TABLE I
PHYSICAL CONSTANTS OF THERMOPILE CONSTITUENTS

	C	ρ	V	K	k
	$J/deg\text{-}g$	g/cm^3	$J/deg\text{-}cm^3$	$10^3 W/cm\text{-}deg$	$10^3 cm^2/s$
(0) Thermal junctions*					
Constantan—manganin	0.41	8.86	3.56	215	60
Constantan—chromel	0.43	8.82	3.79	190	50
(1) Insulation†					
Mylar	1.18	1.40	1.65	1.55	0.95
Kapton	1.10	1.42	1.56	1.55	1.04
Teflon	1.05	2.20	2.30	2.51	1.09
Mica	0.88	3.00	2.64	7.53	2.85
(2) Solution§	4.15	1.00	4.17	5.63	1.35
(3) Muscle§	3.71	1.06	3.92	4.90	1.25

*Calculated from properties of constituent metals, CRC Handbook of Chemistry and Physics, 65th edition.
†Mylar, kapton — physical properties given by the manufacturer. Teflon — as cited by Woledge et al. (1985). Mica — Hill, 1937.
§Hill, 1965.

The inverse transform of $sT_0(0,s)$ is

$$\tau_0 \frac{dT_0(0,t)}{dt} \rightarrow A_{2,3}A_{1,2}A_{0,1}2^3 \frac{1}{\sqrt{4\pi}(t/\tau_0)^{3/2}} e^{-\tau_0/4t} \quad \text{as } t \rightarrow 0. \quad (30)$$

The initial rate of temperature change is limited by the time constant τ_0, which depends on the spatially weighted diffusivities of the layers between the muscle and the center of the thermopile. The impulse in rate of volume heat production causes an initial step change in the temperature at the muscle-insulation interface, $T_3(x_3, t)$, given by $(A_{2,3}\,\Delta q_3/V_3)$. The step in T_3 is propagated through the various layers with a delay, τ_0, that has the same form for 1 to 3 layers. We expect that for n layers the initial delay will depend on the sum of n spatially weighted diffusivities. The volume heat capacities enter as a scale factor in this initial response and have a minor effect on the rate of temperature change.

The final approach to steady state can be determined by expanding $T_0(0, s)$ as $s \rightarrow 0$, then inverting to obtain $T_0(0, t)$ as $t \rightarrow \infty$. The small s expansion can be represented as

$$\frac{\Delta q_3}{sV_3} \rightarrow \frac{1 + \tau_2 s}{1 + \sqrt{\tau_3 s}}$$

$$\xrightarrow{T_3(x_3,s)} \frac{1}{\left(1 + \frac{a^2}{k_0}s\right)\left(1 + \frac{b^2}{k_1}s\right)\left(1 + \frac{c^2}{k_2}s\right)(1 + \tau_2 s)} \rightarrow T_0(0,s),$$

where

$$\tau_3 = \ell_{eff}^2/k_3$$

$$\ell_{eff} = \frac{V_0}{V_3}a + \frac{V_1}{V_3}b + \frac{V_2}{V_3}c$$

$$\tau_2 = \frac{V_0}{V_1}\frac{ab}{k_1} + \frac{V_0}{V_2}\frac{ac}{k_2} + \frac{V_1}{V_2}\frac{bc}{k_2}. \quad (31)$$

For sufficiently small s, the s terms became negligible in comparison to the $\sqrt{s}$ term, and $T_0(0, s) \rightarrow T_3(x_3, s)$. The final time course as $t \rightarrow \infty$ is therefore given by

$$T_0(0,t) = T_3(x_3,t) = \frac{\Delta q_3}{V_3}(1 - e^{t/\tau_3}\text{erfc}\sqrt{t/\tau_3}$$

$$\approx \frac{\Delta q_3}{V_3}\left[1 - \frac{1}{\sqrt{\pi t/\tau_3}}\right], \quad (32)$$

where the erfc is the complimentary Error Function (Abramowitz and Stegun, 1972, 297–298) and the last expression on the right side of Eq. 32 is the asymptotic expansion for large argument.

The final time constant, τ_3, depends on the diffusivity of muscle and the thickness of each layer weighted by its volume thermal capacity relative to muscle. It has the same form as the time constant derived by Hill (1937) based on his approximation of the thermopile as a single homogeneous layer with the diffusivity of muscle and an equivalent half thickness determined by its thermal capacity (see Eq. 34 below and related text).

The physics of heat flow is related to the expansion for small s in the following way. The initial flow of heat from the muscle to the layers of the thermopile causes a drop in the temperature T_3 at the muscle surface, x_3, and an increase in the temperature of the layers. When the temperature of the layers is essentially equal to $T_3(x_3, t)$, we can neglect the terms proportional to s, and the remaining temperature changes are limited by the rate of heat diffusion within the muscle (viz. the term proportional to square root s). The drop in T_3 and the spatial profile of temperature as $x \rightarrow \infty$ depends on how quickly heat diffuses into the cooler layers from the rest of the muscle and is therefore a function of the muscle's diffusivity.

The first order delays introduced by the various finite layers become insignificant in comparison to the diffusion

of heat in the infinite muscle. However, in other systems, better control of the surface temperature (or surface solute concentration or surface voltage) may be possible, in which case the approach to steady state will be limited by these first order delays due to the layers of material.

Fig. 2 illustrates the effects of diffusivity (k) and volume thermal capacity (V) predicted by Eqs. 27–32. We numerically invert the transformed step response (Eq. 26) to obtain an accurate representation of the time response over the entire interval of interest. The step response of one of the thermopiles used by Gilbert and Ford (1988) is shown by solid lines. The symbols show step responses obtained by replacing its mylar insulation with a material having the same V as mylar but a k value twice as high (*diamonds*) or with another material having the same k but a V value twice as high (*triangles*). Comparison of the diamonds with the solid line shows that increasing k speeds up the first 10–20 ms of the step response (*upper panel*) without affecting the tail at long intervals (*lower panel*). Comparison of the triangles and solid line shows that increasing V does not affect the first few milliseconds of the response but lengthens the tail.

Comparison With Hill's Analysis

Specifications of thermopiles given in the literature usually include equivalent half-thickness, which is a measure of thermal capacity. It has also been assumed to provide information about speed, on the basis of Hill's analysis (1937, 1965). Our analysis shows, however, that the assumption can be misleading at short intervals (see Hill, 1965, 325–327). It is therefore useful to compare results of our analysis with Hill's.

Hill's boundary conditions can be applied to Eq. 25. The step response obtained can then be compared with his time-domain response and with the step response computed as described above. Hill assumed the thermopile to consist of a single layer of material having the same thermal diffusivity as muscle. Its thickness, a', the equivalent half-thickness, he defined as that of a layer of muscle having the same thermal capacity as half the thermopile.

$$a' V_3 = aV_0 + bV_1 + cV_2. \tag{33}$$

Note that this intuitive definition of a' yields an expression identical to that derived for ℓ_{eff} in Eq. 31. Hill's step response in the time domain is given by

$$\bar{T}_0(t) = 1 - \text{erf}\,[a'/\sqrt{4k_3 t}]. \tag{34}$$

A direct comparison can now be made between the two analyses: our Eq. 26 takes into account thicknesses and diffusivities of each layer; Hill's Eq. 34 uses equivalent half-thickness and the diffusivity of muscle. Fig. 3 shows step responses computed from our analysis (*lines*) and Hill's (*symbols*) for thermopiles H2 (*diamonds*, described below) and HIL (*triangles*, described by Hill, 1965).

The response of Hill's thermopile as calculated with Eq. 26 is very similar to Hill's approximate analysis. Although he was cautious about the validity of his assumptions at short intervals (see Hill, 1965), these graphs show that the analysis is valid for his instruments at all intervals.

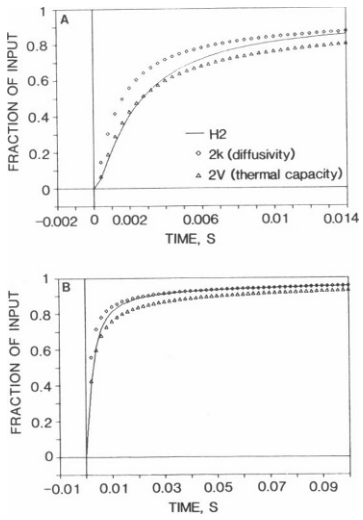

FIGURE 2 Difference in diffusivity and thermal-capacity effects on step response. (*Solid lines,*) H2-thermopile described below. (*Diamonds,*) 2k-thermopile with same dimensions and thermal capacity as H2 but doubled insulation diffusivity. (*Triangles,*) 2V-thermopile with same dimensions and layer diffusivities as H2 but doubled insulation thermal capacity. Responses were computed from Eq. 26 by an IBM XT with a program that numerically converts a function in the s-domain to a one-dimensional array in the time domain. Computation intervals were 0.4 ms in *A* and 2 ms in *B*.

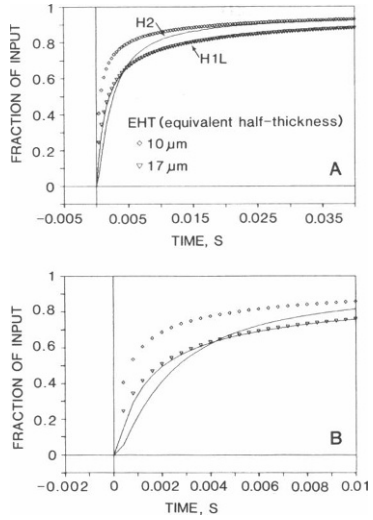

FIGURE 3 Comparison of step responses of thermopiles H2 and HIL computed from Eqs. 26 with two separate layers (*lines*) and 34 (*symbols*) with Hill's boundary conditions (see text). Graph legend: 5 CC, 13 My — H2 with constantan-chromel junctions (half-thickness 5 μm) and mylar insulation (12.7 μm); 7.5 CM, 15 Mi — thermopile described by Hill (1965) with constantan-manganin junctions (half-thickness 7.5 μm) and mica insulation (15 μm). Equivalent half-thicknesses (see text) were 10 μm for H2 and 17 μm for Hill's thermopile, calculated from Eq. 33 and the physical constants of constituents given in Table I.

The initial response of H2 calculated from its equivalent half-thickness (*diamonds*) is faster at short intervals than if the layers are treated separately, although the two curves converge at ~25 ms. The graph in B with the expanded time scale shows that Hill's instrument is somewhat faster than H2 at intervals <5 ms, despite its thicker layers and larger thermal capacity. As shown in Table 1, the diffusivity of the mylar used to insulate H2 is substantially lower than the diffusivities of the junctions, the muscle and the mica with which Hill's instrument was insulated, and it limits the instrument's response at short intervals. The graphs show that the approximations used in his analysis, while valid for his thermopiles, should not be used to describe the early responses of other instruments.

Responses of Modern Thermopiles

Step responses of the two thermopiles used in the study described in the accompanying paper (Gilbert and Ford, 1988) are shown in Fig. 4. Both were constructed of constantan-chromel thermal junctions flattened to a thickness of 10 μm. The junction half-thickness, a, is therefore 5 μm. H2 was insulated with a single layer of mylar (b = 13 μm). H1M had layers of kapton and mylar, each 13-μm thick. In computing Fig. 4 the fluid layer was omitted and for H1M, layers 1 and 2 have the properties of kapton and mylar, respectively. As expected, H2 is considerably faster than H1M at short intervals (graphs with time base 4 ms/division). The two produced similar responses at long intervals (200 ms/division), because the extra layer of insulation only slightly increased the thermal capacity of H1M.

The effect of a layer of solution between the muscle fibers and the thermopile insulation is illustrated in Fig. 5. The response of H2 was computed with a = 5, b = 13, and c = 0 or 10 μm (*squares*). Because the thermal properties of kapton and mylar are similar, we assign layer 1 averaged properties and compute the response of H1M with a = 5, b = 26, and c = 0 or 10 (*diamonds*), the first of these being

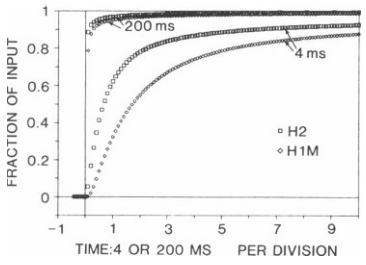

FIGURE 4 Step responses of two thermopiles. Temperature change at center of thermal junctions in response to instantaneous heat produced by the muscles at time t = 0, computed from Eq. 26, the step response in the s-domain. (a) Half-thickness of junctions. (b,c) Thicknesses of inner and outer insulation layers, respectively. Both instruments have constantan-chromel junctions. H2 was insulated with a single layer of mylar 12.7-μm thick, H1M with an inner layer of kapton and an outer layer of mylar, each 12.7 μm. Time scale 4 ms/division (responses ~0.33 and 0.63 at the first division) or 200 ms/division.

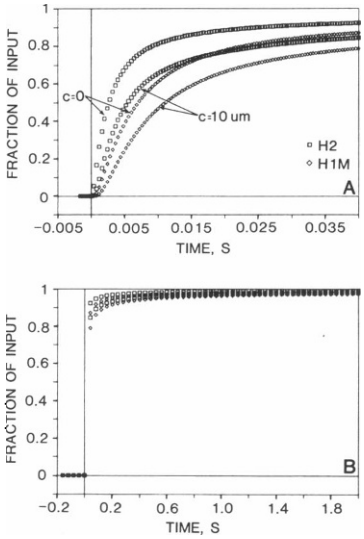

FIGURE 5 Effect of solution layer on step responses. Same instruments and symbols as in Fig. 4. Slower responses of both instruments were obtained by including a solution layer 10-μm thick (*dimension c*). For H1M, the insulation layer was taken to be 25.4 μm thick with physical constants equal to the average of those of mylar and kapton, which are similar (Table I). Its response with c = 0 is identical to that shown in Fig. 4, computed for two insulation layers.

virtually identical to the response computed for a = 5, b = 13, and c = 13 (compare diamonds in Figs. 4 and 5 *A*). Inclusion of the solution layer reduced the step response of H2 at 10 ms from 0.8 to ~0.65 of steady state and of H1M from 0.6 to ~0.47. As expected from Eqs. 27–30, the initial response of H2 with a 10-μm solution layer is faster than that of H1M with no solution layer present. All four responses are at least 95% maximal after 0.5 s.

Response to Transient Heat Production

The transfer function (Eq. 25) can be used to simulate thermopile output in response to any temporal pattern of heat production by the muscles. Simulated responses and muscle records are compared in the accompanying paper (Gilbert and Ford, 1988, Fig. 2). Figs. 6 and 7 show the effects of diffusion delay on transient heat inputs that were of particular interest in that study.

The simulated response to any input is obtained by multiplying the Laplace transform of the input function by the transfer function, Eq. 25. For example, the thermoelastic response of the muscle to a rapid 0.2-mm release can be approximated as (Gilbert and Ford, 1988)

$$\frac{1}{V_3}\int q_3(t)\,dt = u(t)[1.000 + 0.615e^{-500t}] \qquad (35)$$

in which 38% of the heat produced instantaneously is subsequently absorbed. The Laplace transform is

$$\frac{q_3(s)}{V_3 s} = \frac{1}{s} + \frac{0.615}{s + 500}. \qquad (36)$$

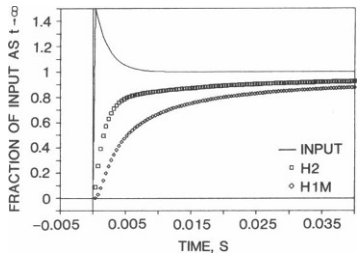

FIGURE 6 Responses of H2 (*squares*) and H1M (*diamonds*) to thermoelastic heat produced by muscles in response to a 1-ms, 0.2-mm release. The input function in the time domain is given by Eq. 36 and approximates the first 20 ms of the expected thermoelastic response. Its Laplace transform is given by Eq. 37 and the inverse transform obtained numerically is shown by the solid line.

The transformed response is the product of Eqs. 25 and 36. Transient responses obtained numerically in the time domain are shown in Fig. 6 for the two thermopiles used by Gilbert and Ford (1988). The transient peak in the input is not seen in the simulated output of either instrument. A thermopile would have to be considerably faster than either H2 or H1M to exhibit such a peak. As shown in Fig. 7, the increase in speed required for the output to show a small transient peak could be produced by insulating the instrument with a thinner layer of mylar (3 instead of 13 μm, [*diamonds*]) or a 6.5-μm layer of mica (*squares*). The step response of such an instrument would be at least 0.4 of the input in 0.4 ms, instead of <0.1, as obtained with H2 and H1M (Fig. 4).

DISCUSSION

The results of the analysis show how the geometry and thermal properties of thermopile components affect response time. The analysis has several applications. It provides a rigorous method for determining the limits of time resolution, allows effects of dimensions and thermal properties of components to be examined individually, and can be used to correct thermopile records for diffusion delay and extract all the available information about rapid heat changes at short intervals.

The time delays due to diffusion through several layers of material are shown to occur on more than one time scale. In a homogeneous medium, the only time scale is the square of the thickness of the medium divided by the diffusivity. A layered medium is therefore fundamentally different from a homogeneous one, and there is no set of effective parameters that will make them equivalent. In the problem studied, the initial temperature changes were limited by diffusion through the layers of material whereas the final approach to steady state was limited by diffusion in the semi-infinite medium. However, if we could eliminate the diffusional delays associated with the semi-infinite phase, the layers of material would still delay the final approach to steady state, and the time constant for the final response would still differ from that for the initial response. For example, if we could achieve a step change in $T_3(x_3, t) = 1$, the initial time constant is given by τ_0 (Eq. 29), whereas the final time constant can be obtained by multiplying out the four first order delays shown just above Eq. 31 and keeping only terms proportional to s. This yields

$$\tau_f = \frac{a^2}{k_0} + \frac{b^2}{k_1} + \frac{c^2}{k_2} + \frac{V_0}{V_1}\frac{ab}{k_1} + \frac{V_0}{V_2}\frac{ac}{k_2} + \frac{V_1}{V_2}\frac{bc}{k_2}$$

and the final approach to steady state is $[1-\exp(-t/\tau_f)]$. Thus the finite layers will give an exponential approach to steady state whereas an infinite medium depends on $1/\sqrt{t}$ as given in Eq. 32. Moreover, the final time constant, τ_f, depends on the volume heat capacities, but if any two of the dimensions go to zero (e.g., $b = c = 0$), then the dependence on heat capacity drops out, the medium becomes homogeneous, and $\tau_0 = \tau_f$.

The limits of time resolution have been examined by allowing the transfer function to operate on various patterns of heat production by muscles. Simulated responses to input functions with transient peaks are particularly interesting. Whether observable evidence of a peak appears in the response of a particular instrument depends on the size of the input peak and the speed of the instrument. One thermopile used in this laboratory is fast enough to produce a transient peak in response to a particular input, while another is not. Although the peak is not apparent in the latter's response, it is contained in the kinetics of that response and appears when the response is corrected for diffusion delay, as shown in the accompanying paper (Gilbert and Ford, 1988, Fig. 3).

Examination of the flow of heat through layers of material produced one result that is particularly significant for rapid myothermic measurements. The thermal capacities of thermopiles, in the form of equivalent half-thicknesses, are usually specified in the literature, whereas the diffusivities of component materials are rarely mentioned. This analysis shows that the diffusivities determine the speed of the early response, while thermal capacity has little effect. Moreover, the criteria for initial speed, namely high diffusivity, may lead one to choose a material that has a slow final reponse. For example, from Table I, mica has the highest thermal diffusivity of the insulation materials listed, but it also has the largest volume heat capacity,

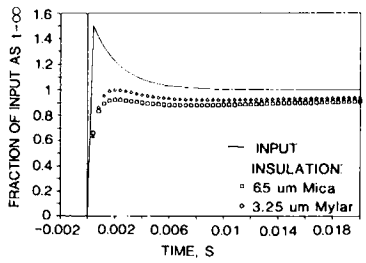

FIGURE 7 Expected responses of faster thermopiles to same input (*solid line*) shown in Fig. 6. (*Squares*) mica insulation 6.5-μm thick, (diamonds) mylar insulation 3.25-μm thick.

which will produce the slowest final response. For the thermal junctions, constantan-manganin has the highest diffusivity and lowest heat capacity, so it is clearly the best choice.

It follows that thermopile design can be optimized for specific applications. The kinetics of heat changes on a millisecond time scale could be measured more reliably by thermopiles insulated with materials with high thermal diffusivities. For example, the metal-film instruments developed by Mulieri et al. (1977) for small single preparations like papillary muscles are constructed by vacuum deposition of metals onto thin sheets of mica, whose diffusivity is high. Such an instrument, modified for use with pairs of sartorius muscles, would be considerably faster than those currently employed.

The initial objective of the analysis was to derive a transfer function which can be used to correct thermopile records for diffusion delay. By treating the layers of the system separately, it is possible to determine their effects on the interpretation of corrected records. A case in point is the extra solution layer whose thickness is not easily measured. As shown in the following paper, a set of transfer functions computed with several thicknesses of this layer is used to simulate a set of responses to a known input. The simulated responses are compared with a muscle record to establish the probable range of layer thickness. The records are then corrected with transfer functions whose thicknesses lie within this range, to determine the effect of layer thickness on the interpretation of the records.

The analysis has not yet been applied to other temperature-measuring systems. The transfer function derived here is appropriate for the rapid stopped-flow calorimeter described recently by Howarth et al. (1987). It measures heat produced by a solution of contractile proteins in contact with both sides of a thermopile element, and the boundary conditions are the same as those used here. Boundary conditions must be modified to derive transfer functions for other preparations, such as single-muscle fibers (Curtin et al., 1983) or papillary muscles (Mulieri et al., 1977), which rest only on one side of the thermopile.

We would like to thank Nancy Walker and Elizabeth Bain for typing and editing the typescript, and Bob Butz for assistance with the computer programming.

This work was supported in part by National Science Foundation grants PCM-7911748 and PCM-8120276, the Muscular Dystrophy Association, the Georgia Heart Association, and National Institutes of Health grants HL36075 and EY06391.

Received for publication 17 November 1987 and in final form 16 May 1988.

REFERENCES

Abramowitz, M., and I. A. Stegun. 1972. *Handbook of Mathematical Functions.* Dover Publications, Inc., Mineola, New York.

Curtin, N. A., J. V. Howarth, and Roger C. Woledge. 1983. Heat production by single fibers of frog muscle. *J. Musc. Res. Cell Motil.* 4:207–222.

Gilbert, Susan H., and Lincoln E. Ford. 1988. Heat changes during transient tension responses to small releases in active frog muscle. *Biophys. J.* 54:611–617.

Hill, A. V. 1937. Methods of analyzing the heat production of muscles. *Proc. R. Soc. Lond. B. Biol. Sci.* 124:114–136.

Hill, A. V. 1965. *Trails and Trials in Physiology.* Williams & Wilkins, Baltimore, MD.

Howarth, J. V., N. C. Millar, and H. Gutfreund. 1987. A stopped-flow microcalorimeter for biochemical applications. *Biochem. J.* 248:677–682.

Mulieri, L. A., G. Luhr, J. Trefry, and N. R. Alpert. 1977. Metal-film thermopiles for use with rabbit right ventricular papillary muscles. *Am. J. Physiol.* 233:C146–C156.

Woledge, Roger C., Nancy A. Curtin, and Earl Homsher. 1985. *Energetic Aspects of Muscle Contraction.* Specific heats of materials. Table 4.II, p. 175.